



## Accelerated carbonate biomineralisation of Venetia diamond mine coarse residue deposit (CRD) material – A field trial study

Thomas Ray Jones <sup>a,\*</sup>, Jordan Poitras <sup>a</sup>, Alan Levett <sup>a</sup>, Andrew Langendam <sup>b</sup>, Andrew Vietti <sup>c</sup>, Gordon Southam <sup>a</sup>

<sup>a</sup> School of Earth & Environmental Sciences, The University of Queensland, St. Lucia, QLD 4072, Australia

<sup>b</sup> The Australian Synchrotron (ANSTO), Clayton, Victoria 3168, Australia

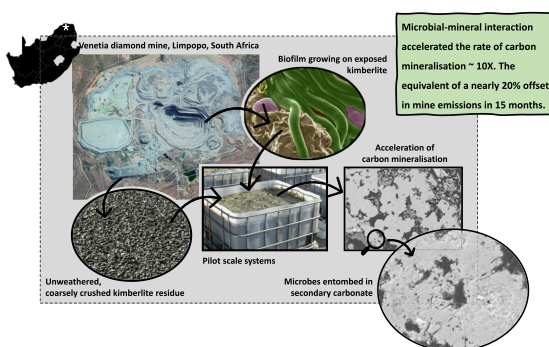
<sup>c</sup> Vietti Slurrytec, Johannesburg, 1684, South Africa



### HIGHLIGHTS

- Kimberlite and rainwater supported growth of photosynthetic biofilms.
- Cyanobacterial biofilms accelerated kimberlite weathering, leading to increased pedogenesis and plant growth.
- Biogeochemical activity accelerated mineral carbonation of within coarse residue deposit (CRD) kimberlitic material.
- A 2 wt.% increase in carbonate (ca. 20% mine site CO<sub>2</sub>e offset) was observed at surface conditions after 15 months.

### GRAPHICAL ABSTRACT



### ARTICLE INFO

Editor: Daniel CW Tsang

#### Keywords:

Kimberlite  
Mineral carbonation  
Photosynthetic biofilm  
Technosol  
Carbon capture and storage

### ABSTRACT

Field trials combining mined kimberlite material (Coarse Residue Deposit; CRD) and mine derived microbes show accelerated kimberlite weathering at surface conditions – a potential method for accelerated carbon sequestration via mineral bio-carbonation. A photosynthetic biofilm suspension (20L), sourced from the Venetia diamond mine (Limpopo, South Africa) pit wall, was cultured in 3 × 1000 L bioreactors using BG-11 medium. Bioreactors supplemented with Fine Residue Deposit (FRD) kimberlite material enhanced microbial growth and kimberlite weathering. This (ca. 1.44 kg) wet weight bio-amendment corresponded to ca. 1.5 × 10<sup>9</sup> *Acidithiobacillus* spp. sized bacteria/g CRD (20 kg FRD growth supplement + 60 kg FRD used for harvesting biomass + 850 kg CRD used in the field trial experiment). This bio-amendment promoted carbonate precipitation and subsequent cementation under surface conditions (0–20 cm). Microbial inoculation accelerated pedogenesis of CRD materials. A soil-like substrate resulted from weathering under environmental conditions in Johannesburg from January 2020 to April 2021. Over this 15-month experiment, the biodiversity found in the inoculum shifted due to the selective pressure of the kimberlite. The natural, endogenous biosphere, when combined with the inoculum, accelerated carbonate precipitation in the upper 20 cm of the bioreactor by between +1 wt% and +2 wt%. Conversely, carbonation of the bioreactor at depth (20–40 cm) decreased by ca. 1 wt%. All the secondary carbonate observed in the bioreactors was biogenic in nature, i.e., possessing microbial fossils. This secondary carbonate took the form of both radiating acicular crystals as well as colloform intergranular cements. This microbial inoculum and resulting geochemical changes promoted the transformation of kimberlite into a Technosol, capable of supporting the germination and growth of self-seeding, windblown grasses, which enhanced weathering in the rhizosphere. The maximum secondary carbonate production is consistent with a ca. 20 % mine site CO<sub>2</sub>e offset.

\* Corresponding author.

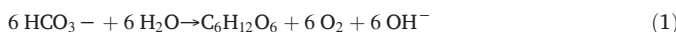
E-mail address: [t.jones@uq.edu.au](mailto:t.jones@uq.edu.au) (T.R. Jones).

## 1. Introduction

The ever-mounting threat of climate change via the anthropogenic input of greenhouse gases into the atmosphere has resulted in the increasing expectation of companies to lower their carbon footprint (IPCC, 2021). This can most efficiently be achieved by tailoring specific methodologies to best suit the processes and environment of the intended sequestration system, aiming to reduce costs and increase carbon sequestration. The ultramafic mineralogy and vast on-site processing capabilities of diamond mines are an important criterion for carbon sequestration, making these sites plausible targets for mineral carbonation (Mervine et al., 2018).

Most of the carbon on Earth is housed in stable minerals that are derived directly or indirectly from the chemical weathering of other minerals. Known as mineral carbonation, this form of carbon sink has the capacity to store 106 Gt of carbon world-wide for an indefinite length of time (Lackner, 2003). Mineral carbonation is the formation of stable carbonates by the reaction of CO<sub>2</sub> with naturally occurring minerals, usually containing magnesium, iron, and calcium (Rackley, 2017). This geochemical process occurs naturally over geological time, and at an accelerated rate within ultramafic kimberlite lithologies. The ultramafic mineralogy of kimberlites is highly susceptible to weathering at Earth's surficial conditions. This trait, used historically to aid in the mining of diamonds, makes this material an attractive candidate for mineral carbonation - and the Venetia mine, an excellent natural laboratory and case study for possible on-site carbonation (Field et al., 2008). The kimberlite currently mined at Venetia is from below this weathering horizon; therefore, if paired with weathering processes that break-down primary minerals and promote the precipitation of secondary carbonates, this kimberlite could serve as a host for a large-scale carbon sequestration program to offset mine emissions.

The ability of microorganisms to dissolve and precipitate minerals is well documented and employed in many industrial and environmental settings. This has led to the development of biotechnological processes in the mining and environmental remediation industries, utilising complementary biogeochemical cycles (Brandl and Faramarzi, 2006; Dupraz et al., 2009; Gadd and Raven, 2010; McCutcheon et al., 2017; Power et al., 2011). Microbe-mineral interactions dominate surface and sub-surface geochemical cycling, via organic and inorganic acid weathering (Southam, 2012), providing cations for carbon sequestration. Under Earth's surface conditions, microorganisms utilise different metabolic strategies to generate energy and biomass, which affect carbon cycling. Photoautotrophic microorganisms (Eq. (1)) are critical to mineral carbonation. Their drawdown of CO<sub>2</sub> via HCO<sub>3</sub><sup>-</sup> serves as a conduit for continued carbonate mineralisation by forming hydroxy anions, which draws CO<sub>2</sub> from the atmosphere (Eq. (2)), producing bicarbonate (Eq. (3)) forming carbonates with divalent cations (Eq. (4); Baumgartner et al., 2006; Jones et al., 2023a; Krumbein, 1974).



The process by which photoautotrophic microorganisms induce carbonate minerals is well understood and widely observed, with nearly 70 % of the carbonate rocks on Earth being formed by, or by the influence of, cyanobacteria (Altermann et al., 2006). These microbes, along with the microbes utilised in this field trial, often exist as biofilms. A biofilm comprises of a group of microbes, known as a consortium, that exist in a syntrophic mass - adhering to both each other and to a surface (López et al., 2010). These cellular aggregates produce a binding matrix composed of extracellular polymeric substances (EPS) which house the consortium.

Mineral carbonation is dependent on the available cations, a source of inorganic carbon and environmental pH. The mineral substrate where

any proposed acceleration in mineral carbonation is to occur must be susceptible to mineral dissolution, releasing cations capable of spontaneous mineral formation with CO<sub>3</sub><sup>2-</sup> (Eq. (3)). Kimberlites are 'one' such substrate, with well-known low-temperature alteration reactions occurring during yellow ground formation, where the resulting carbon sequestration occurs via the formation of secondary carbonate minerals (see Bodéan et al., 2014; Jones et al., 2023a; Jones et al., 2023b; Power et al., 2013; Sparks, 2013; Wilson et al., 2009). This geochemical evolution; accelerated weathering and precipitation; pushes this altered material to be classified as an anthropized soil, specifically, a Technosol. These soils are the product, in some way, of human intervention – such as the extraction of materials not normally under the influence of surficial processes, i.e., mined materials (IUSS Working Group WRB, 2015; Morel et al., 2015).

This study is part of Project CarbonVault™, an initiative undertaken by De Beers with the aim of lowering the carbon footprint of their diamond mines via accelerated carbon mineralisation. Our research is focused on the microbial processes at play in weathering kimberlitic residue that has been processed to reflect industry standards. Specifically, can these processes be accelerated in a way that accelerates secondary carbonate mineral formation (Jones et al., 2023a). Microbially induced carbonate precipitation (MICP) could be a viable method by which CarbonVault™ sequesters CO<sub>2</sub>, with additional potential benefits of microbial carbonation includes tailings stabilisation and soil regeneration, improving rehabilitation. If existing mining activity can be paired with biosequestration of carbon, kimberlitic 'mine waste' from a single mine could offset hundreds of millions of tonnes of CO<sub>2e</sub> emissions annually.

## 2. Materials and methods

### 2.1. Field site, sample collection and bacterial culture work

The materials used for this field trial were sourced from the Venetia diamond mine, Limpopo, South Africa (22°25'59" S, 29°18'50"E) (Fig. 1A). The Venetia kimberlite group is made up of 12 occurrences: 11 pipes, and 1 intrusive dyke (Allsopp et al., 1995). The mine is South Africa's largest diamond producer, liberating ~4.2 million carats in 2018, and processing 4.74 Mt. of kimberlite in 2016 (Mervine et al., 2018). The kimberlite currently being extracted and processed from Venetia is dominated by phyllosilicates, primarily serpentine minerals and smectites (19.0 wt% and 36.6 wt%, respectively), with diopside present at an average abundance of 20.5 wt% (Mervine et al., 2018).

The mine area contains the pit, the Fine Residue Deposit (FRD), and the Coarse Residue Deposit (CRD) tailings storage facilities. The two kimberlite residue deposits refer to two different size fractions produced by the diamond extraction process, with the FRD hosting the ≤ 800 μm grain size fraction, and the CRD hosting the 800 μm – 8 mm grain size fraction.

#### 2.1.1. Venetia microbes and bioreactor setup

Microbial biofilm, associated water, and kimberlitic material attached to biofilm were collected into two 20 L buckets from the Venetia pit. Fifteen kilograms of 'biofilm' was collected into each bucket towards the base of the active pit, i.e., below the groundwater table, in area K1, benches 29 and 30 (Fig. 1B-E). The buckets were transferred from the Venetia mine to the De Beers Group Technology SA facility in Johannesburg where it was homogenised and divided between six bioreactors that were each filled with 1000 L of an augmented BG-11 medium (Ripka et al., 1979). Sodium carbonate (Na<sub>2</sub>CO<sub>3</sub>) was removed from the medium to limit the potential transport of this carbonate ion into the experimental system upon inoculation. To promote growth, an enriched medium was created based on the cumulative addition of 10-fold strength BG-11 medium, divided and applied over the four-month incubation period. Three bioreactors were used in this experiment.

#### 2.1.2. Kimberlite material

Bulk kimberlite material was collected directly from the Venetia mine Run of Mill (ROM; September 2019) and transported to the De Beers

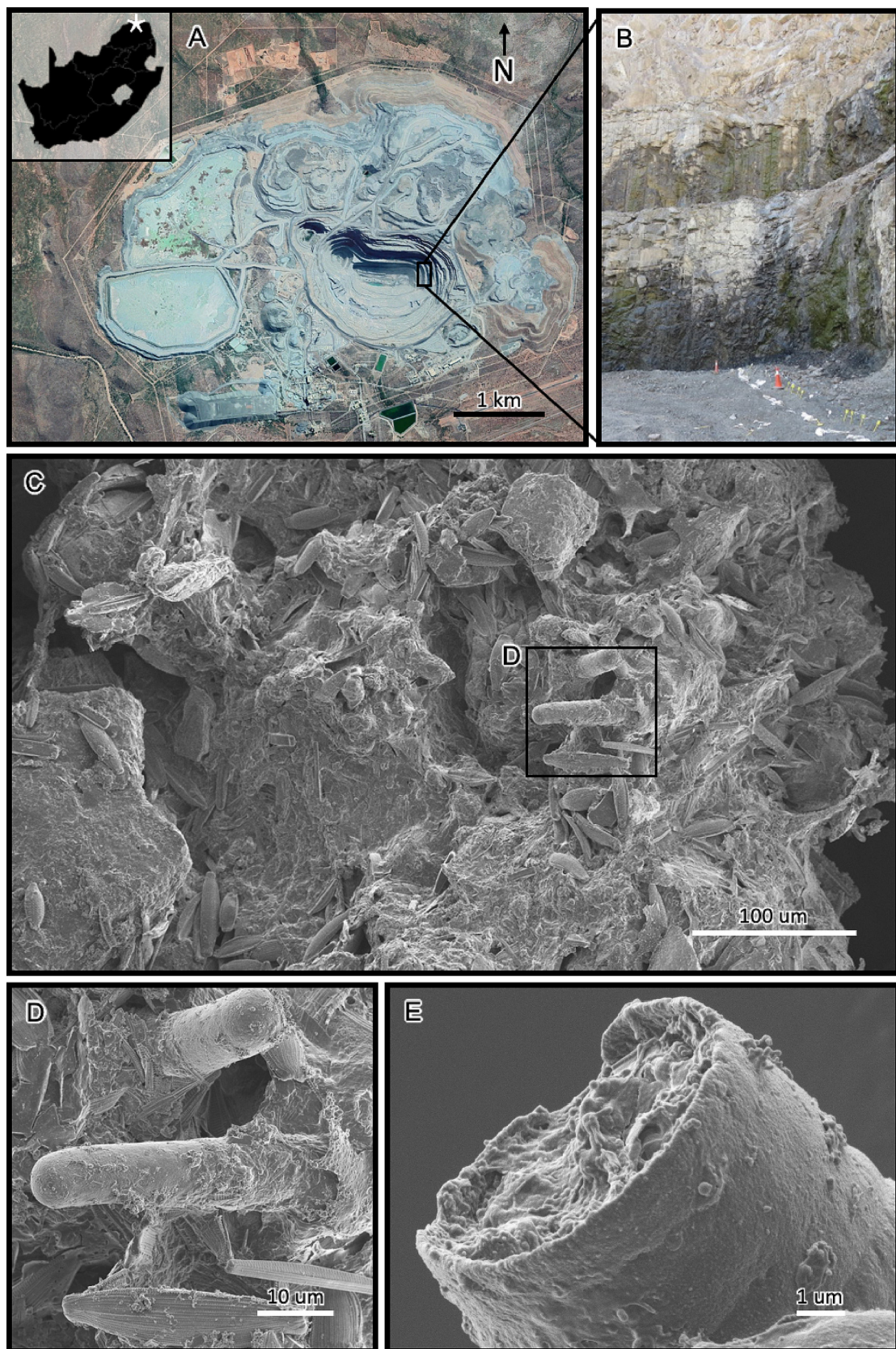


**Fig. 1.** A) A Google Earth satellite image of the Venetia diamond mine, Limpopo, South Africa, its location indicated by the star on the inset image ( $22^{\circ}25'59''$  S,  $29^{\circ}18'50''$  E) of South Africa. B) Benches 29 and 30 as viewed from the pit floor (K1 – East), showing water seepage through the kimberlite and the location of a well-established biofilm that was sampled for use in the field trial experiment. Tiles C and D display secondary electron SEM images of the biofilm, showing a diverse microbiome (bacteria, cyanobacteria, fungi, and diatoms) that has coated and intermixed with kimberlite. E) A large cyanobacterium (*Oscillatoria* sp.) growing at surface of the biofilm-kimberlite composite.

Group Technology SA research facility where it was crushed and screened to a Venetia CRD grain size (0.8–8 mm) for use in this trial. The systems were set-up in Intermediate bulk containers (IBCs), combining kimberlitic material +/− inoculation with Venetia microorganisms (biofilm – microbial mats) (Fig. 2).

#### 2.1.3. Growth and harvesting microbial mats

To concentrate/de-water the microbial biomass generated in the bioreactors, 20 kg of high surface area, <800 µm FRD kimberlitic material was added to each bioreactor to initiate and aid in the aggregation and settling of the biomass. After 24 h settling of the kimberlite-biomass composite, ca. 90 % of the spent culture media was removed, leaving the microbial biomass FRD-kimberlite mix on the floor of each bioreactor tank.

#### 2.1.4. CRD-microbe mixing and experiment deposition

'Homogenous' conditions: 850 kg of unweathered CRD material was split equally and mixed into the three de-watered bioreactors and mixed thoroughly using shovels. This material (CRD (850 kg) + FRD (60 kg) + wet weight biofilm + water = 1213 kg) was then transferred into the IBC representing  $T = 0$  (January 2020) for the weathering experiment (Fig. 2A). The level of the CRD-water interface stabilised after 24 h, further dewatering the experimental system via settling, which allowed us to remove an additional 56 L of clear liquid by gravity after opening the valve

at the bottom of the IBC, leaving 307 kg of biofilm + water. To allow for vadose conditions in the IBC, comparable to the CRD residue pile, the stop-cock at the bottom of the IBC was left open.

#### 2.1.5. Control system

A control system was run alongside the inoculated field trial experiment. This was achieved through the transfer of 850 kg of dry CRD into an IBC along with the continuous addition of 363 L of city water to mimic the initial water saturation within the biotic experiment. This control system was also left open to create vadose conditions. After deposition and settling, the CRD levels within the inoculated and non-inoculated 1 m<sup>3</sup> IBCs were roughly 50 cm deep. Both IBCs were trimmed to ca. 60 cm height to allow exposure to sun and rain (weathering conditions) and access for sampling (Fig. 2).

#### 2.2. Sampling

Samples of surface kimberlite from both the inoculated- and control-systems were sampled and transferred into sterile 50 cc Falcon tubes over the course of the experiment:  $T = 0$  (January 2020);  $T = 4$  months (May 2020);  $T = 9$  months (October 2020); and  $T = 15$  months (April 2021). Material sampling from the surface layer was initially done using a 70 % (vol./vol.) ethanol cleaned trowel. However, an ethanol-cleaned pick/



**Fig. 2.** A) A photograph of the inoculated (left) and non-inoculated (control; right) Coarse Residue Deposit (CRD) systems at  $T = 0$ . Photographs of the inoculated (B) and control (C) systems after 1 year, with the biological plot exhibiting the growth of self-seeded grasses demonstrating the formation of a Technosol.

hammer was needed at 15 months because a mineral cement had reinforced the inoculated CRD kimberlite grains, binding them together.

At 15 months, a depth profile was collected from both systems using a 60 mm diameter aluminium pipe that was repeatedly hammered into the material in the IBC, measured for depth, and withdrawn, bringing material to the surface. The surface layer represents the top 10 cm of the system, and the three subsequent depths are composites of material in each underlying 10 cm layer. To minimise the edge effect all samples were collected towards the middle of the IBC, avoiding previous, surface sample sites (Fig. 2).

### 2.3. Chemical analyses

Major oxides were measured in the surface material (0–10 cm) collected at each time point ( $T = 0, 4, 9$  and 15 months) and from each depth sample collected at 15 months (as above) (Supps. A & B). Ten g sub-samples were collected from each sample, oven dried @ 45 °C for 1 week, then crushed using an agate mill to ca. 100 µm grain size. ICP-OES of the digested samples was undertaken using an Optima 8300DV ICP-OES. Total Organic Carbon (TOC; ALS) analyses were performed to estimate the bacterial inoculum.

### 2.4. Material embedding and lapidary for BSE-SEM, MLA and XFM analyses

Materials collected from the IBC experiments were transported in 50 cc Falcon tubes, then oven dried at 40 °C for 24 h before being dehydrated using 3 × 100 % ethanol treatments. The embedding procedure was done in the transport tube to maintain any natural, in-situ intergranular cements and structures that existed before sampling. Each sample was then embedded sequentially, with two resins. LR White, a hydrophilic resin was used initially as it was unlikely that these clay-rich materials were completely devoid of water; 10 mL of this resin was allowed to flow through the samples by gravity, three times prior to setting anaerobically at 60 °C for 48 h. Once hardened, Epo-Tek 301 resin was vacuum infiltrated to further ensure the rigidity and strength required for sample polishing. Each of the samples were then cut and formed into sections ~150 µm thick to ensure the stability of the biogenic carbonate/cements.

### 2.5. Synchrotron X-ray fluorescent microscopy (XFM) & mineral liberation analysis (MLA)

Elemental mapping of the 150 µm thick slides were mapped using the XFM Beamline at the Australian Synchrotron, Clayton, Australia (Paterson et al., 2011). A monochromatic 18.5 KeV X-ray beam was focused to 2 µm using a Kirkpatrick-Baez mirror pair. Overview scans were run with 20 µm pixels, which were decreased to 2 µm for high resolution maps captured by a 384 element Maia detector (Siddons et al., 2014). Image data was analysed using GeoPIXE (Ryan et al., 2014) to produce elemental maps of the experimental systems. Mineral Liberation Analysis (MLA) was performed on the same samples used for XFM analysis, using a Quanta 600 (Thermofisher) with EDAX SiLi detectors, 3 µm spot size; all MLA processing was done using MLA Dataview v.3. software.

### 2.6. Scanning Electron Microscopy of bio-materials

Material preparation for secondary electron Scanning Electron Microscopy (SEM) analysis was fixed with 2.5 % glutaraldehyde for 24 h at 4 °C. All samples were then dehydrated using an ethanol dehydration series (20 %, 40 %, 60 %, 80 %, 3 × 100 %), and dried using a hexamethyldisilizane series with 100 % ethanol (1:3, 2:2, 3:1, 4:0). Prior to microscopy, samples were placed in a vacuum oven overnight @ 40 °C, plasma cleaned (Evactron Plasma Cleaner) and carbon coated (Quorum Q150T carbon coater). Field Emission Scanning Electron Microscopy (FE-SEM) was undertaken on a JEOLJSM – 7100F at an accelerating voltage of 20 keV for back scattered and between 2 and 4 keV for secondary electron imaging with a working distance of 10 mm.

### 2.7. DNA sampling, extraction, sequencing, and analysis

Sterile, 15 cc Falcon tubes were filled with material from each sampling position and submerged in LifeGuard® Soil Preservation Solution (Qiagen) prior to transport from Johannesburg to Australia. Using a laminar flow cabinet, 0.5 g subsamples were taken from each system using a sterile, clean spatula and sent for DNA extraction at the Australian Centre for Ecogenomics, The University of Queensland. Cell lysis was achieved by bead beating, followed by DNA extraction using DNeasy PowerSoil Pro Kit (#47016, Qiagen, Germany). Amplification of the V6-V8 portion of the 16S rRNA gene, using the universal primer set 926f (5'-TCGTCGGCA GCGTCAGATGTGTATAAGAGACAGAACTYAAAKGAATTGRCGG-3') and 1392wR (5'-GTCTCGTGGGCTCGGAGATGTGTATAAGAGACAGACGGCG GTGWGTRC-3') with modifications to contain the Illumina specific adapter sequence. To prepare libraries, workflow methods outlined by Illumina (#15044223) were used with the exception that the NEBNext® Ultra™ II Q5 Mastermix (New England Biolabs #M0544) was used in standard PCR conditions. DNA purification was achieved using Agencourt AMPure XP beads (Beckman Coulter, Brea, CA, USA). Purified DNA was indexed using Illumina Nextera XT 834 sample Index Kit A-D (Illumina FC-131-1002, San Diego, CA, USA) in the mastermix to assign unique 8-bp barcodes. Equimolar concentrations of the indexed amplicons were pooled before sequencing using a MiSeq instrument with paired-end sequencing (Illumina, San Diego, CA, USA) with a 600-cycle V3 300-bp reads. Total read counts ranged from 3325 to 76,064 reads, with inoculated biological samples containing an average of 58,777 reads. The inoculated control samples had far fewer total reads, only averaging 11,895 reads, indicating a lower biomass in the control system.

Briefly, Cutadapt (v. 3.5) was used to remove the universal primer sequences (Martin, 2011). Reads were subsequently duplicated and filtered using QIIME2 (v. 2022.2), with chimeras removed by DADA2 (-p-2 trunc-len-f 250 and -p-trunc-len-r 230) (Callahan et al., 2017). The resulting amplicon sequence variants (ASVs) were taxonomically assigned using the nonredundant SILVA database (v. 138, clustered at 99 % identity) (Quast et al., 2013). Amplicon data filtration and analyses were performed in R (v. 4.1.3). The following ASVs were discarded: sequences not classified below the phylum level, sequences classified as chloroplasts or mitochondria, sequences not determined to be either archaeal, bacterial or fungal in origin, and ASVs with an abundance of <0.1 %. Heatmaps of top 5 ASVs per sample with a minimum abundance of 3 % were produced using GGplot.

## 3. Results

### 3.1. Technosol formation

Weathering, resulting from the addition of the inoculum to the CRD material promoted the growth of self-seeding native grasses on the crushed kimberlite (Fig. 2), which must have been deposited via aeolian processes as no seeding was performed (Fig. 2B). In contrast, the control system was exposed to the same environmental conditions, but it did not support the growth of plants over the 15-month experiment (Fig. 2C). The associated roots from this vegetation were predominantly found in the upper 20 cm horizon (Fig. 6), although roots were observed in the deeper sections of the system.

### 3.2. Chemical analyses

The geochemical trends of the solids remained relatively similar in the experiments' surface samples over the duration of the experiment. More Fe and Al remained in the biotic system over time as compared to the control, though the opposite is true for Mg, which was shown to weather out at a higher degree in the inoculated column (Supp. A). The oxides from the depth profile read in a similar manner, with the gross trends remaining relatively similar between the control and biotic systems (Supp. B). Total organic carbon analyses of the control and inoculated systems at the

commencement of the experiment equalled 0.026 % and 0.176 %, respectively demonstrating that the inoculum represented 0.15 % TOC. Using the mass of 910 kg kimberlite (850 kg CRD + 60 kg FRD), and the mass of *Acidithiobacillus ferrooxidans* as a model weathering bacterium (Enders et al., 2006), the biologically treated CRD was inoculated with ca.  $1.5 \times 10^9$  bacteria/g CRD. Loss-on-ignition, consistent with biological materials, increased in both systems over time, with the highest concentration seen in the biotic system after 15 months.

### 3.3. Early-stage mineral weathering and carbonation

XFM of the inoculated system revealed an increase in micrometre-scale element heterogeneity (Fig. 3AB) in as little as 4 months. This evidence of chemical and physical CRD weathering coincided with the development of secondary biogenic carbonates observed using high resolution BSE-SEM. Weathering of the large, discrete grains observed at  $T = 0$  resulted in the depletion of these distinct grain boundaries as the intergranular areas became populated with weathering by-products (small breakaway fragments). This increases elemental heterogeneity across the samples over time. The biogenic carbonate was defined by the presence of abundant microbial fossils throughout this material (Fig. 3C). These colloform carbonate clusters appear to link CRD grains to one another - possibly a precursor to the carbonate cements seen in more developed systems (Jones et al., 2023a).

### 3.4. Carbonate

MLA mapping was used to measure the in-situ carbonate wt% within the experimental CRD materials. Both calcite and ankerite were combined to track the total changes in carbonate across the different layers after 15 months (Fig. 4). The total carbonate within the non-inoculated control system was shown to increase at ~1 wt% at surface conditions, though they remained relatively unchanged in the underlying deeper layers. In contrast, the biotic treatment is shown to have a dramatic effect on carbonate weathering and precipitation, with the carbonate in the surface layers increasing by ~2 wt% (0–10 cm) and ~1.5 wt% (10–20 cm). However, the opposite was seen at depth (from 20 cm–40 cm; Fig. 4), where the addition of the inoculum was shown to decrease the amount of carbonate.

After 15 months, regions possessing abundant carbonation were observed as newly developed carbonate clusters (diameter ~10  $\mu\text{m}$ ; Fig. 5B), alongside larger clusters of carbonate (diameter ~100  $\mu\text{m}$ ; Fig. 5C) that must have undergone multiple growth phases if its origins were as ca. 10  $\mu\text{m}$  grains.

### 3.5. Later-stage mineral weathering and carbonation

MLA mapping of the inoculated CRD system after 15 months showed a more widespread dispersal of new secondary carbonate. This carbonate, like that observed in the 4-month sample (Fig. 3), grew between CRD grains

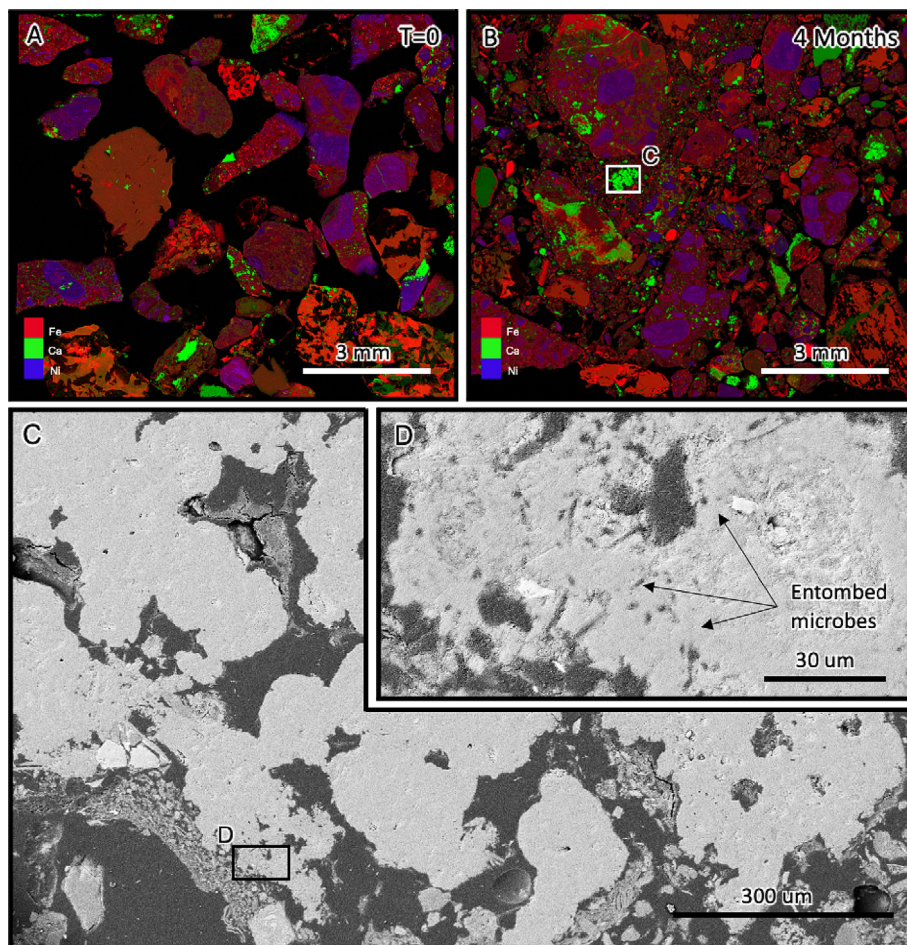


**Fig. 3.** XFM of the CRD field trial study at  $T = 0$  (A) and after 4 months (B) shows dramatic weathering and dissemination of the primary kimberlitic material, along with the growth of rapid growth of mm-scale secondary calcium rich minerals. (C) BSE SEM these calcium precipitates are newly formed carbonate minerals exhibiting multiple nucleation sites, growing in places where weathering, (represented by fine-grained particles infilling between larger grains and the surrounding low atomic mass clay minerals) is active. (D) High-resolution BSE-SEM imaging revealed entombed microorganisms throughout the secondary carbonates, suggesting a microbiological role in carbonate precipitation. The impact of weathering on the CRD material, which evolves from grains being primarily intact and with clear intergranular separation at  $T = 0$ , to having disseminating weathering fronts around each grain, and with and interconnecting cement binding the grains together ( $T = 15$  months).

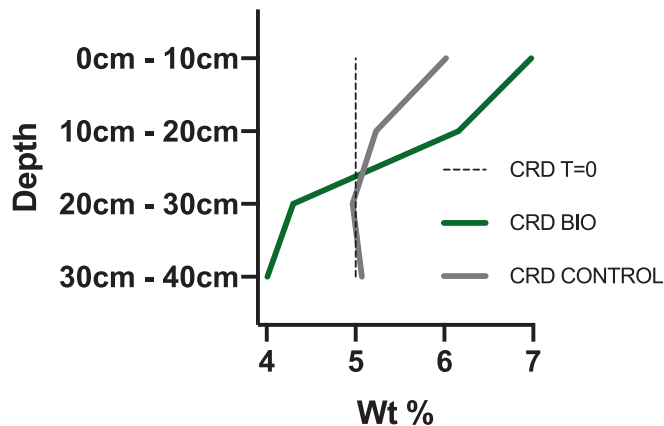


**Fig. 4.** MLA derived wt% of carbonate (as calcite + ankerite) across the CRD depth profile at 15 months. The control experiment increased carbonate at surface conditions (~1 wt%) while remaining relatively unchanged at depth. The microbiological treatment dramatically increased the carbonate at surface (~2 wt%) and near-surface (~1.5 wt%) conditions, though decreased in carbonate at depth.

producing decimetre-scale aggregated ‘hand samples’ that required the use of a hammer to excavate (data not shown; Fig. 6A in thin section). Evidence of repeated mineral nucleation indicates the beginnings of a widespread carbonate-cement-forming environment, accelerated by microbial inoculation. The later-stage carbonate often maintained the generally amorphous-looking colloform structure, though at their periphery these mineral aggregates often possessed acicular radiating carbonates (Figs. 6 & 7).

Tiles 1 and 1a (Fig. 6) show this spherical carbonate mineralogy possessing entombed bacteria, fossilised diatoms, and roots; all of which

were absent in the control system. Roots were common in the upper layers of the microbially treated CRD system, associated with the extensive growth of grass. No plants, nor any associated roots, were present in the control system. Tiles 2 and 2a (Fig. 6) show sections of secondary carbonate, again in weathering fronts, exhibiting layered colloform structures (an early-stage concretion) and acicular radiating carbonates. Tiles 3 and 3a (Fig. 6) show the growth of multiple carbonate grains expanding out and in-between grains; the initiation of wide-spread intergranular cements. XFM visualisation of this region, including Tile 3, demonstrated that dissolution of strontium produced a natural tracer, which lit up the secondary carbonate (presumed aragonite based on acicular habit).

### 3.6. Carbonate growth habit

Two distinct ‘forms’ of biogenic carbonate were observed in every sample. When carbonate growth occurred along a weathering front on kimberlite grains, space limitation causes the formation of tightly packed, colloform carbonate structures (Fig. 7A & C). However, when carbonate nucleation occurred in gaps between CRD grains where space limitations did not exist, it allowed for the growth of large radiating, acicular aragonite (Fig. 7B & D). The presence of microbial fossils is consistent throughout all secondary carbonate forms, demonstrating a role of microorganisms in catalysing the formation of these carbonates. Some areas also demonstrated an intermingling of both, granular/blocky colloform carbonate plus the acicular aragonite.

### 3.7. Microbial community

The surface of the uninoculated (native control) system was initially dominated by *Proteobacteria* (61 % at 0 months ( $T = 0$ ) and 81 % at 3 months ( $T = 1$ )) and *Actinobacteriota* (27 % at 0 months and 17 % at 4 months) (Supp. D). Between 4 and 9 months, the microbial community

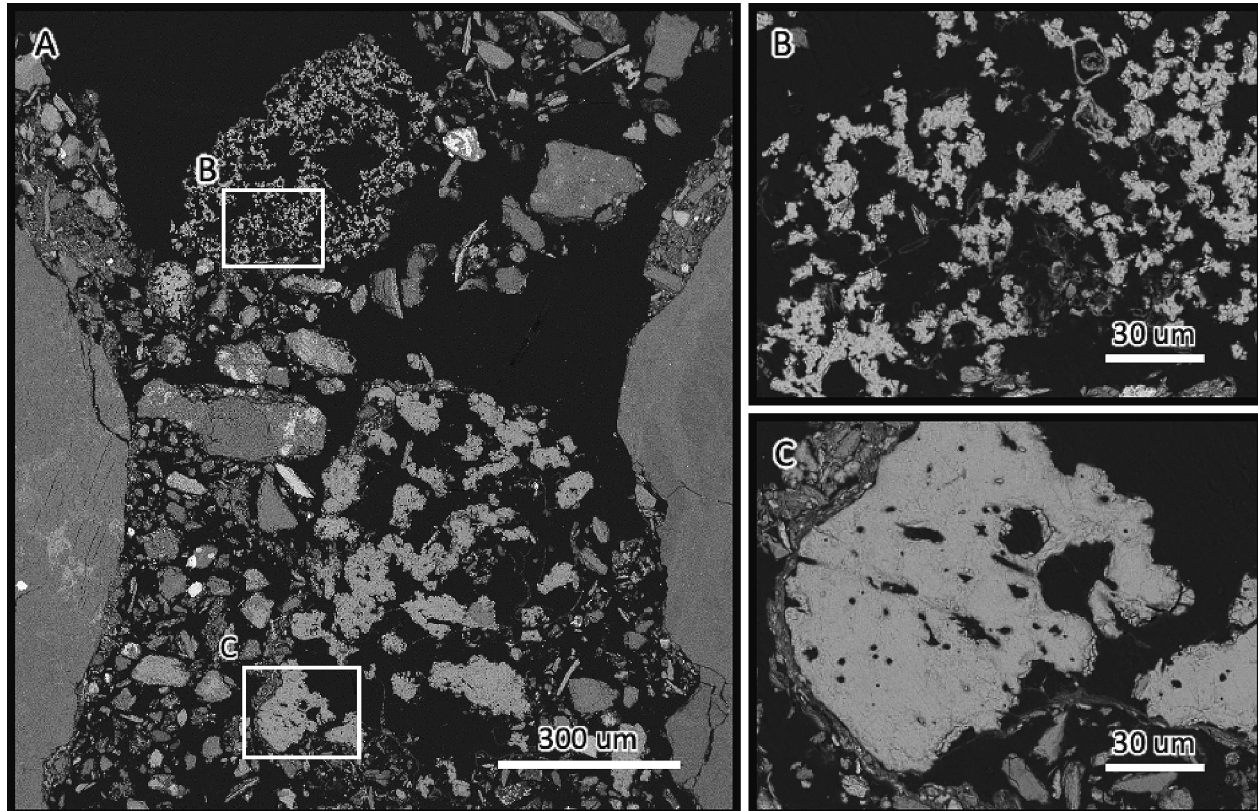
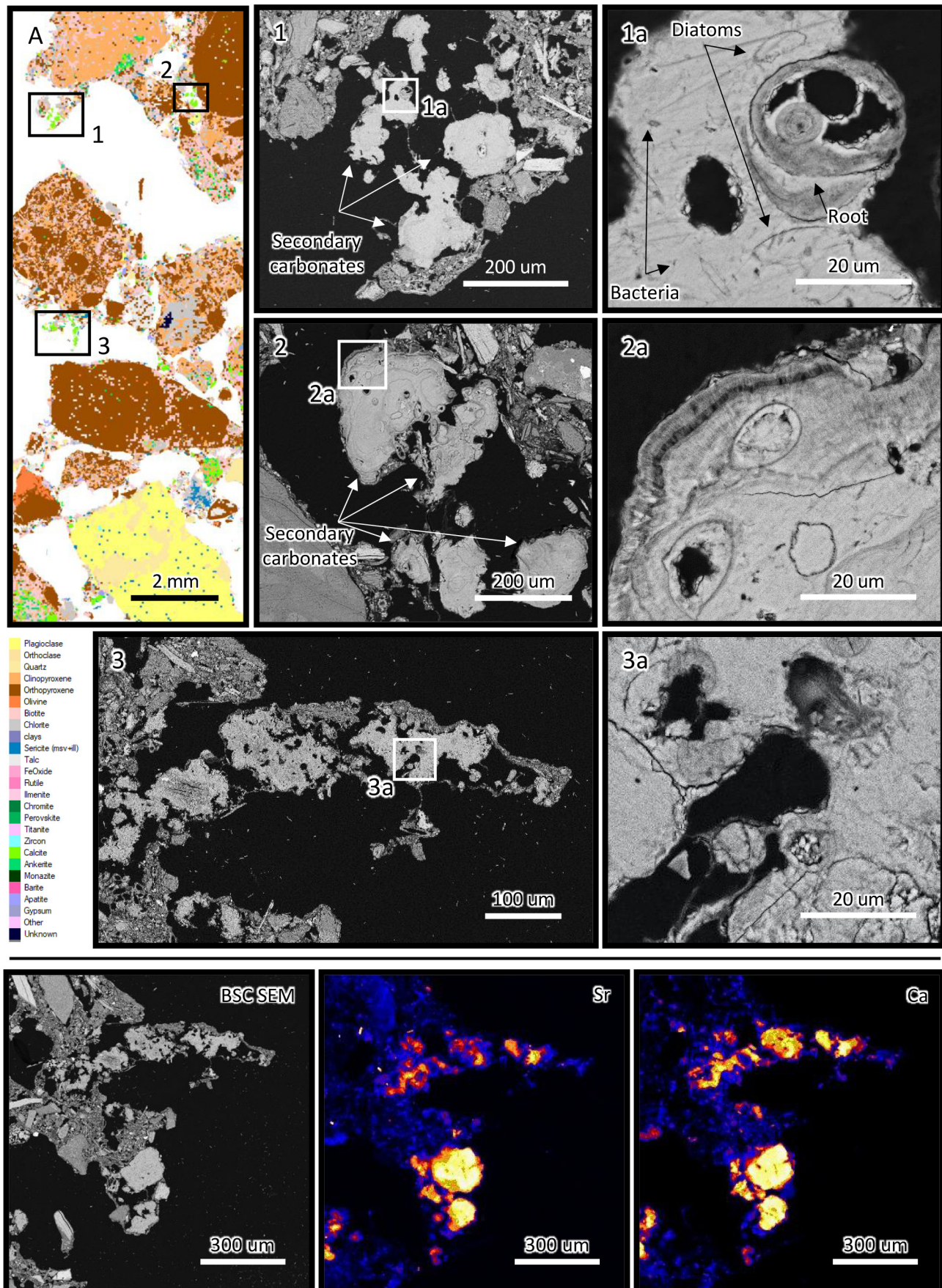


**Fig. 5.** Back-scatter SEM micrograph of the biological system after 15 months showing wide-spread carbonation and exhibiting different size classes, interpreted as newly developing carbonate clusters (mineral diameter ~10  $\mu\text{m}$ ; Fig. 5B), alongside larger/older carbonate clusters that have undergone >1 growth phase (mineral grain diameter ~100  $\mu\text{m}$ ; Fig. 5C).



underwent a drastic shift at the Phylum level, with the uninoculated system becoming dominated by Firmicutes (88 % at 9 months and 67 % at 15 months). At 15 months, a similar microbial community structure at the Phylum level was recorded for all surface and depth (10–20 cm, 20–30 cm and 30–40 cm) samples (Supp. D). The inoculated system had a much greater diversity at the Phylum level with five phyla >5 % found in all surface samples and the grouped ‘Other’ microbial phyla ( $\leq 3\%$  abundance) making up >4 % of each sample. Cyanobacteria typically comprised <1 % of the microbial community, aside from at  $T = 0$ , where the inoculation was introduced and increased the population proportion to 11 %. At the phylum level, the inoculated system generally increased in Firmicutes and Actinobacteria with time after the initial inoculation at the expense of Proteobacteria (Supp. E). Interestingly, after 15 months, the Phragmoplastophyta proportion of the microbial community increased to 6 % of the microbial population at the surface and up to 17 % of the population at depths below 20 cm. The Phragmoplastophyta are likely to be photosynthetic microalgae, though it is unclear if they were living or dead in subsurface samples.

At the genus level, there were few overlapping ASVs between the uninoculated (Supp. C) and inoculated systems (Fig. 8). The uninoculated CRD materials were initially dominated by *Pseudomonas* and *Georgina* ASVs at the surface until  $T = 4$  months. From 4 to 15 months, the uninoculated system was dominated by *Bacillus* and *Lactobacillus*, both at surface and depth. The uninoculated system initially contained a small proportion of a *Desulfosporosinus* ASV, a putative anaerobic sulphate-reducing microorganism. At the 15-month depth profile sampling, ASVs of *Exiguobacterium* and *Hymenobacter* were present, microorganisms previously identified in oligotrophic and extreme environments, including Dry Valley in Antarctica (Marizcurrena et al., 2019) and within mealworm guts fed polystyrene (Yang et al., 2015). At the genus level, the inoculated system was also initially dominated by a *Pseudomonas* ASV, replaced by a *Bacillus* ASV as the experiment proceeded, both at surface and depth (Fig. 8). After 15 months, the inoculated system also increased the relative proportion of ASVs with the Rhizobiaceae family and ammonium oxidising archaea, *Candidatus Nitrosocosmus*, which may contribute to supporting soil formation, and plant germination and survival in the microbiologically inoculated system (Pessi et al., 2022; Sadowsky and Graham, 1998).

## 4. Discussion

### 4.1. Soil evolution

The evolution of the inoculated, weathered CRD material is best highlighted by the prominent growth of native, windblown grasses (Fig. 2). Visually, this IBC is in stark contrast to the untreated CRD material, which did not support the growth of plants. This represents a clear acceleration in the transformation of the CRD from a crushed primary material into a weathered soil-like material (Technosol; Ruiz et al., 2020; Xiaofang and Huang, 2014) possessing increased secondary minerals, including biogenic aragonite (Figs. 5–7). The correlation between environmental chemistry (Supps. A & B), the bacterial populations, and the dynamic response of the bacteria to the different, environmental growth conditions demonstrates that the type of inoculum, and how these microbes interact with the mineral substrates are more important than simply including a soil microorganism to the process. This was particularly evident in the control system, that showed minimal evidence of mineral dissolution, soil generation and no plant development, though interestingly it still possessed a diverse microbiome supported by kimberlite as a growth substrate (Supp. C). Given the relatively small population of bacteria in the control

system these bacteria must have been growing under limiting environmental conditions, imparted by the kimberlite. The consortia collected from the Venetia pit was selected due to the precursory environmental acclimatisation it had experienced. Allowing it to overcome the growth limiting environmental conditions that slowed microbial activity in the control.

### 4.2. Microbially enhanced weathering

The release of primary cations from the parent kimberlite material is an essential step in mineral carbonation as they are needed to pair with the carbonate ions to form stable minerals. This cation release/extent of weathering is evident after 15 months as the originally ‘clean’ CRD grains at  $T = 0$  have developed assorted intergranular cements (Figs. 5–7) and where the source of these new, secondary materials can only be derived from the primary CRD clasts.

Though the microbially treated system showed a higher degree of weathering and mineral breakdown, bulk ICP (oxide; Supps. A & B) analysis of the systems showed that the Al, Fe, and Ca was seen at higher levels than the control after 15 months. This was perhaps due the widespread trapping and binding abilities of exopolymeric substances produced during growth of the microbial inoculum in the bioreactor as well as during growth in the IBC during weathering. The fine-grained materials produced during weathering, even as early as 4 months (Fig. 3AB), also became trapped in the surrounding biofilm and/or became entrapped during secondary carbonate precipitation. A strong indicator that weathering, i.e., the simultaneous breakdown of primary minerals and precipitation of secondary material was occurring, was provided by the strontium signal, which was ‘lost’ from the weathered kimberlite and taken up by the secondary aragonite, providing an endogenous tracer for weathering and carbon dioxide sequestration. This alkali earth metal, which is ubiquitous in Earth’s crust (average = 450 ppm), may prove useful for tracking carbonate precipitation and in validating biologically catalysed carbon dioxide sequestration. Strontium can replace calcium in the precipitation of aragonite, a biogenic calcium carbonate, providing an indicator of biogenicity (Banner, 1995; McCutcheon et al., 2017). The secondary, biogenic carbonates produced throughout the inoculated CRD contain a consistent, prominent strontium signature (Fig. 6), indicating a high degree of localised kimberlite weathering was taking place, releasing strontium, which was incorporated into microbial carbonate.

### 4.3. Microbial impact on carbonate

Biogenic carbonate was found across the entire depth profile in both experimental systems. Where it was most prominent in the upper 20 cm of the system (Fig. 6), several 100’s of  $\mu\text{m}$  in diameter secondary carbonate mineral aggregates were observed (Figs. 5–7). These carbonates housed remnant biological material, i.e., fossilised bacteria, diatoms, and roots. Carbonate growth was predominantly situated in the highly weathered inter-granular sections of the CRD system, where the fine-grained material provided a high surface area and the abundant cations which can help support microbial growth. This highly localised growth degraded the surrounding primary minerals:

1. creating a constantly accelerating weathering pattern,
2. providing further cations for carbonation,
3. increasing microbial activity, and
4. providing the nucleation points and preferred geochemical conditions for carbonate formation.

**Fig. 6.** A) An MLA scan of a sample from the inoculated CRD field trial exp. (surface) after 15 months. The development of carbonate (calcite/ankerite) is visible on the weathering margins of the primary minerals (Opx/Cpx/Ol). The biogenic nature of the carbonates is shown via the presence of fossilised bacteria, diatoms, roots (1, 1a), and banded growth rings (2, 2a). These microbially induced minerals represent the initiation of carbonate cementation within the CRD system, the binding and trapping nature of which is clearly shown in tiles 3 and 3a, where the growth of the secondary carbonate is aggregating with the weathered mineralogy/clay minerals. Imaging the tile 3 region using XFM demonstrated that Sr provided a natural tracer to identify weathering and secondary carbonate formation, presumably as aragonite.

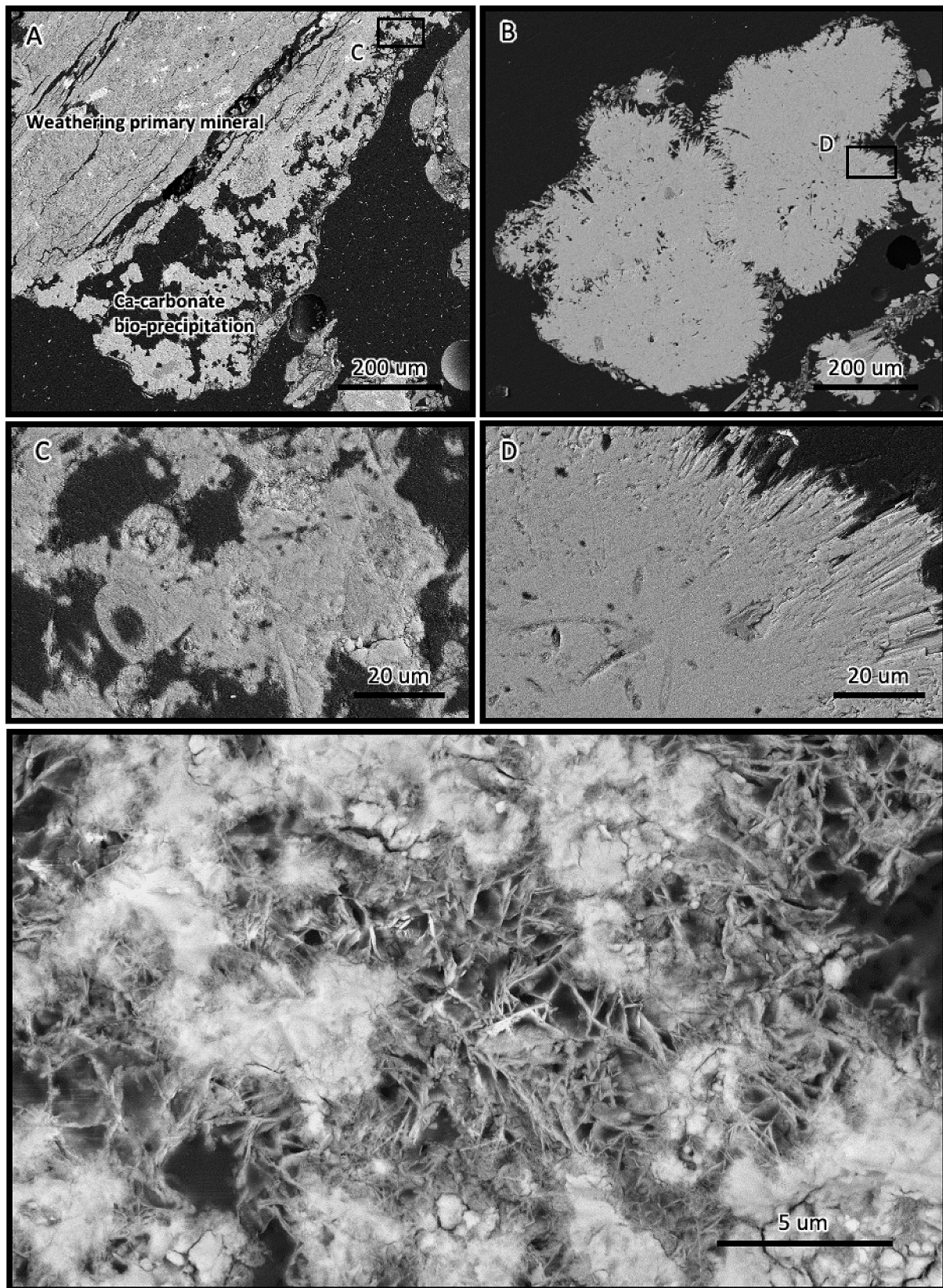


**Fig. 7.** Back-scatter SEM showing two styles of carbonate mineral carbonation within the inoculated CRD system. A) Shows the development of carbonate material at the weathering front of a heavily disseminated Si-mineral with a biofilm-clay slurry distally encompassing the mineral. This carbonate shows the development of a blocky mineral structure. With no spatial limitations, the carbonate is shown to grow large, radiating acicular minerals (B). High resolution micrographs of both styles (C & D) of precipitation shows numerous fossilised microbes within the carbonate. E) An area of biogenic carbonate showing an intermingling of granular/blocky carbonate mineral forms, and acicular/radiating forms.

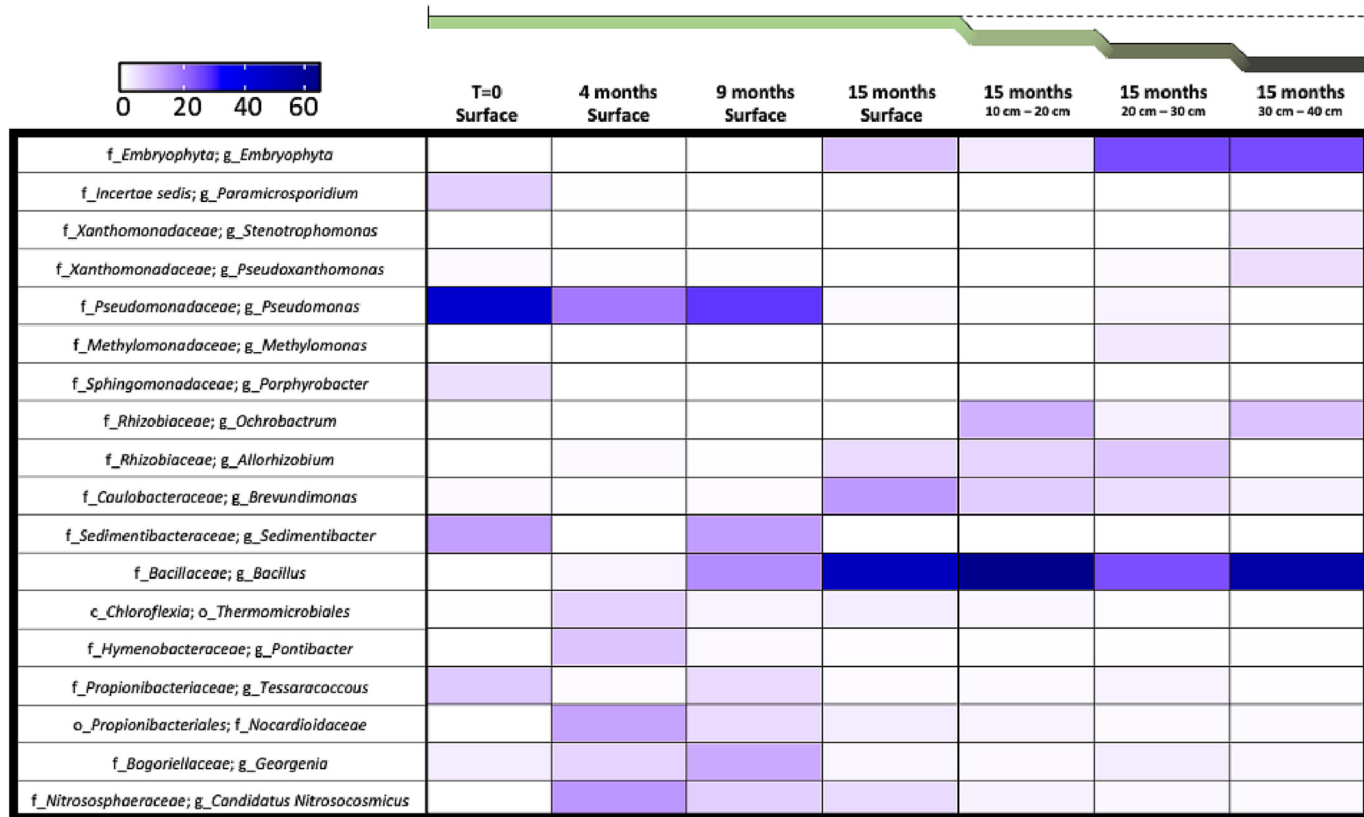


**Fig. 8.** Mean relative abundance of the most abundant genera (or lowest resolved taxonomic level) with an abundance of 3 % or more across all Course Residue Deposit (CRD) materials in the inoculated (B) system for the initial setup (T0), and surface (0–10 cm) subsampling at 4 months (T4), 9 months (T9) and 15 months (T15). After 15 months, a depth profile was collected, including subsamples from 10 to 20 cm, 20–30 cm and 30–40 cm. Diagram at the top of the figure visually represents sampling depth.

Microbial weathering of the kimberlite aided in the precipitation of carbonate under surface conditions through it appears to have hindered the growth of carbonate under deeper (> 20 cm) near-surface conditions. This is likely due to the ‘removal’ of the photosynthetically driven oxygen production at depth, resulting in the microbial population shifting from an aerobic/photosynthetic/heterotrophic consortium to an anaerobic/fermenting (acid producing) population. This population change is the likely precursor to the depletion of carbonate at depths of >20 cm in the biogenic experiment (Fig. 4). Interestingly, this weathering of carbonate did not correspond to a decrease in CaO (Supps. A & B), suggesting that the calcium is still available within the system to promote carbonation. This indicates the need to either: 1 - capture and recirculate any fluids from the lower sections to the more reactive surface horizons (0–20 cm), or 2 - seal off the system to promote further weathering and anaerobic respiration conditions in a saturated environment, which achieved a 27.1 % mine offset carbonation equivalent under laboratory settings (Jones et al., 2023b).

#### 4.4. Microbial population changes through time

Microbial population shifts over time were prominent in both systems, even in the inoculated system. The population of photosynthetic microbes on which this mineral carbonation method was based receded over time as other common soil microorganisms arose and dominated the environment. This trend was predicted and pre-emptively addressed via the addition of kimberlite to the bioreactor to create a selective pressure and assure a dominant kimberlite-eating inoculation once transferred into the kimberlite experiment – though this proved of little benefit in terms of maintaining a dominant cyanobacteria population. Photosynthesis was maintained throughout the system, though through the presence of a photosynthetic microalgae *Phragmoplastophyta*, which likely aided in mineral carbonation. The selective pressure of the kimberlite, paired with the

abundant microbes already existing in the kimberlite material (and its' surrounding environment) drove population shifts more so than the inoculation, though the final populations were not the same between the inoculated and non-inoculated systems – demonstrating that the additions of microbes had an impact on the final microbiome. It is likely that the same processes that accelerate mineral bio-carbonation are still active in the control, just at a slower rate – giving further credence to the use of microbial inoculation as an accelerant.

#### 4.5. Potential for mine emission offsets

The 2 to ~1.5 wt% carbonate values (calcite + ankerite; MLA) across the upper 20 cm CRD depth profile demonstrates that there is a near surface catalyst enhancing weathering and mineral carbonation, which may be derived or driven by the grasses and the rhizosphere. A 2 wt% increase in calcium carbonate within this CRD system indicates that 8.8 g CO<sub>2</sub>e/kg of kimberlite has been sequestered. If this 2 wt% benchmark seen at surface conditions can be reproduced across the entire Venetia mine treated ore (4.74 Mt. in 2016) (Mervine et al., 2018), this would see the sequestration of 41,712 t of CO<sub>2</sub>e within the mined material (Jones et al., 2023b) – correlating to an offset in mine emissions of approximately 20 %.

Weathering in this ‘plant system’ has an increase in cost due to the loss of water via evapotranspiration (Maschinski et al., 1999). As an alternative, the increase in carbonate under surface conditions (~1 wt%) in the control system, given the relatively low amount of biomass, is remarkable. When combined with the carbonate values remaining relatively unchanged at depth, i.e., no loss of carbon from the system, this may provide the best overall strategy for carbon mineralisation at mine sites.

As the CRD breaks down over time, it will improve its water holding capacity, which has demonstrated the ability to enhance carbonation under anaerobic conditions at depth in the laboratory (Jones et al., 2023b).

This CO<sub>2</sub>e offset would also hold economic value in regard to carbon tax benefits and Cap-and-Trade Allowances. The 2022 carbon tax rate in South Africa was R\$144 (US\$7.5)/tCO<sub>2</sub>e, with plans to increase annually by consumer price inflation (CPI) + 2 % until 2025 (Carbon Tax Act, 2019). This price will continue to increase beyond 2025. The High Level Commission on Carbon Prices, released by the C.P.L. Coalition (2019), has recommended that in order to see real change, this price should be increased to US\$50–100/tCO<sub>2</sub>e by the year 2030. As this price increases, so too will the economic value of mineral carbonation - with those able to sequester their own CO<sub>2</sub> standing to gain over those who can't.

#### 4.6. Rate of carbonate vs historical CRD material

The increase in secondary carbonates within kimberlite residue mimics the natural evolution of blue-ground kimberlite to yellow-ground kimberlite that occurs when kimberlite is exposed to surface conditions. This change has also been observed in CRD material from historically mined kimberlite. CRD material from the Cullinan diamond mine in Gauteng, South Africa, was shown to have developed an inter-granular carbonate cement in the ~50 years since its deposition, originally as loose CRD clasts (Jones et al., 2023a). The secondary carbonate within the Cullinan CRD that developed over ~50 years accounts for ca. 16.39 wt% of the sample. Though the precise rate of carbonate precipitation at Cullinan could not be measured, in an effort to provide an estimate it was assumed that carbonation was continuous through time and that, like Venetia, it contained ~5 wt% primary carbonate. By dividing the increase (wt%) in carbonate by the years since deposition, it was shown that the secondary carbonate within the Cullinan CRD increased ~0.228 wt% each year. Using this same method, it can be determined that the inoculation of the Venetia CRD kimberlite (at surface conditions) precipitated carbonate at a rate roughly 10 x that estimated for the Cullinan mine CRD.

## 5. Conclusion

The addition of a microbial consortia, soured from the Venetia mine, to crushed CRD kimberlite residue accelerated the development of secondary carbonate in this mined material, while transforming the kimberlite into a Technosol. The mineral carbonation rate measured under surface conditions within the CRD field trial occurred at a rate roughly 10 x faster than carbonation seen in non-inoculated, historically mined kimberlites, and was equivalent to a mine emission offset of nearly 20 %. Though the population of microbes originally added into the system were shown to change over time, the microbial treatment accelerated the establishment of wind-blown grass seeds - demonstrating the initiation of Technosol formation via the weathering of kimberlite, which did not occur in the control system. A biotechnological approach seems to provide a simple, successful, and generally hands-off approach to accelerating mineral carbonation. There are several streams of potential (further) work within this area, including developing a better understanding of carbonation with depth, and a refinement of processes/conditions/microorganisms for increased weathering and carbonation. However, potentially achieving a ca. 20 % offset in mine emissions within 15 months is a significant step in understanding how mined kimberlite can be utilised to lessen the impact of mining in ultra-mafic material. Mineral carbonation is a natural phenomenon often occurring over geological time – the strategic addition of microbes into ex-situ kimberlite material can accelerate this rate to align with the more pressing timeframe of human-driven sustainability efforts.

## Ethical approval

NA

## Funding

Financial support was provided by De Beers Group Services RSA Pty Ltd. and the Australian Nuclear Science and Technology Organisation.

## CRediT authorship contribution statement

T.R.J was involved in conceptualisation, field work, designed and initiated the experiments, performed analysis and data curation, wrote the manuscript, and prepared all figs. J.P. aided in field work, experiment set-up and DNA analysis. A. Levett aided in DNA analysis and data curation. A. Langendam contributed to the XFM work. A.V aided in experiment up-keep, sampling, and logistics. G.S. was involved in project/experiment conceptualization and initiation, funding acquisition, field work, experiment design/set up, and document review.

## Data availability

Data will be made available on request.

## Declaration of competing interest

I report a relationship with De Beers Group Services RSA Pty Ltd. that includes: funding grants.

## Acknowledgements

This work was funded by De Beers project CarbonVault™. Field work was supported by Henry May of Slurrytech, Johannesburg, South Africa. Part of this research was undertaken on the ANSTO XFM beamline at the Australian Synchrotron. SEM was carried out at the Centre for Microscopy and Microanalysis at University of Queensland. MLA was performed by Elaine Wightman at the Julius Kruttschnitt Mineral Research Center (JKMRC) within the Sustainable Minerals Institute (SMI), UQ. Geochemistry samples were measured using a Perkin Elmer Optima 8300DV ICP-OES in the Environmental Geochemistry Laboratory, UQ.

## Appendix A. Supplementary data

Supplementary data to this article can be found online at <https://doi.org/10.1016/j.scitotenv.2023.164853>.

## References

- Allsopp, H.L., Smith, C.B., Seggie, A.G., Skinner, E.M.W., Colgan, E.A., 1995. The emplacement age and geochemical character of the Venetia kimberlite bodies, Limpopo Belt, northern Transvaal. *S. Afr. J. Geol.* 98, 239–244.
- Altermann, W., Kazmierczak, J., Oren, A., Wright, D.T., 2006. Cyanobacterial calcification and its rock-building potential during 3.5 billion years of earth history. *Geobiology* 4 (3), 147–166.
- Banner, J.L., 1995. Application of the trace element and isotope geochemistry of strontium to studies of carbonate diagenesis. *Sedimentology* 42, 805–824.
- Baumgartner, L.K., Reid, R.P., Dupraz, C., Decho, A.W., Buckley, D.H., Spear, J.R., Przekop, K.M., Visscher, P.T., 2006. Sulfate reducing bacteria in microbial mats: changing paradigms, new discoveries. *Sediment. Geol.* 185 (3–4), 131–145.
- Bodénan, F., Bourgeois, F., Petiot, C., Augé, T., Bonfils, B., Julcour-Lebigue, C., Guyot, F., Boukay, J., Tremosa, J., Lassin, A., 2014. *Ex situ* mineral carbonation for CO<sub>2</sub> mitigation: evaluation of mining waste resources, aqueous carbonation processability and life cycle assessment (Carmex project). *Min. Eng.* 59, 52–63.
- Brandl, H., Faramarzi, M.A., 2006. Microbe-metal-interactions for the biotechnological treatment of metal-containing solid waste. *China Particuology* 4 (2), 93–97.
- C.P.L. Coalition, 2019. Report of the High-Level Commission on Carbon Pricing and Competitiveness.
- Callahan, B.J., McMurdie, P.J., Holmes, S.P., 2017. Exact sequence variants should replace operational taxonomic units in marker-gene data analysis. *ISME J.* 11 (12), 2639–2643.
- Carbon Tax Act (Act No. 15 of 2019), 2019. Environmental, Climate and Sustainable Development Laws. South Africa. ZAF-2019-L-108806.
- Dupraz, C., Reid, R.P., Braissant, O., Decho, A.W., Norman, R.S., Visscher, P.T., 2009. Processes of carbonate precipitation in modern microbial mats. *Earth-Sci. Rev.* 96 (3), 141–162 Vancouver.
- Enders, M.S., Knickerbocker, C., Titley, S.R., Southam, G., 2006. The role of bacteria in the supergene environment of the Morenci porphyry copper deposit, Greenlee County, Arizona. *Econ. Geol.* 101, 59–70.
- Field, M., Stiefenhofer, J., Robey, J., Kurszlaukis, S., 2008. Kimberlite-hosted diamond deposits of southern Africa: a review. *Ore Geol. Rev.* 34, 33–75.
- Gadd, G.M., Raven, J.A., 2010. Geomicrobiology of eukaryotic microorganisms. *Geomicrobiol. J.* 27 (6–7), 491–519.
- IPCC, 2021. Climate Change 2021: The Physical Science Basis. Contribution of Working Group I to the Sixth Assessment Report of the Intergovernmental Panel on Climate

- Change. In: Masson-Delmotte, V., Zhai, P., Pirani, A., Connors, S.L., Péan, C., Berger, S., Caud, N., Chen, Y., Goldfarb, L., Gomis, M.I., Huang, M., Leitzell, K., Lonnoy, E., Matthews, J.B.R., Maycock, T.K., Waterfield, T., Yelekçi, O., Yu, R., Zhou, B. (Eds.), Cambridge University Press, Cambridge, United Kingdom and New York, NY, USA <https://doi.org/10.1017/9781009157896> (In press).
- IUSS Working Group WRB, 2015. World reference base for soil resources 2014, update 2015. International soil classification system for naming soils and creating legends for soil maps. World Soil Resources Reports No. 106.
- Jones, T.R., Poitras, J., Paterson, D., Southam, G., 2023a. Historical diamond mine waste reveals carbon sequestration resource in kimberlite residue. *Chem. Geol.* 617, 121270.
- Jones, T.R., Poitras, J., Paterson, D., Gagen, E.J., Southam, G., 2023b. Accelerated mineral bio-carbonation of coarse residue kimberlite material by inoculation with photosynthetic microbial mats. *Geochem. Trans.* 24, 1. <https://doi.org/10.1186/s12932-023-00082-4>.
- Krumbtein, W.E., 1974. On the precipitation of aragonite on the surface of marine bacteria. *Naturwissenschaften* 61, 167–168.
- Lackner, K.S., 2003. A guide to CO<sub>2</sub> sequestration. *Science* 300 (5626), 1677–1678.
- López, D., Vlamakis, H., Kolter, R., 2010. Biofilms. *Cold Spring Harb. Perspect. Biol.* 2 (7), a000398.
- Marizcurrena, J.J., Herrera, L.M., Costabile, A., Morales, D., Villadoniga, C., Eizmendi, A., Davyt, D., Castro-Sowinski, S., 2019. Validating biochemical features at the genome level in the Antarctic bacterium *Hymenobacter* sp. strain UV11. *FEMS Microbiol. Lett.* 366 (14).
- Martin, M., 2011. Cutadapt removes adapter sequences from high-throughput sequencing reads. *EMBnet. J.* 17 (1), 10–12.
- Maschinski, J., Southam, G., Hines, J., Strohmeyer, S., 1999. Efficacy of subsurface constructed wetlands using native southwestern U.S. plants. *J. Environ. Qual.* 28, 225–231.
- McCutcheon, J., Nothdurft, L.D., Webb, G.E., Shuster, J., Nothdurft, L., Paterson, D., Southam, G., 2017. Building biogenic beachrock: visualizing microbially-mediated carbonate cement precipitation using XFM and a strontium tracer. *Chem. Geol.* 465, 21–34.
- Mervine, E.M., Wilson, S.A., Power, I.M., Dipple, G.M., Turvey, C.C., Hamilton, J.L., Vanderzee, S., Raudsepp, M., Southam, C., Matter, J.M., Kelemen, P.B., Steffenhofer, J., Miya, Z., Southam, G., 2018. Potential for offsetting diamond mine carbon emissions through mineral carbonation of processed kimberlite: an assessment of De Beers mine sites in South Africa and Canada. *Mineral. Petrol.* 112, 755–765.
- Morel, J.L., Chenu, C., Lorenz, K., 2015. Ecosystem services provided by soils of urban, industrial, traffic, mining, and military areas (SUITMAS). *J. Soils Sediments* 15, 1659–1666.
- Paterson, D., de Jonge, M.D., Howard, D.L., Lewis, W., McKinlay, J., Starratt, A., Kusel, M., Ryan, C.G., Kirkham, R., Moorhead, G., Siddons, D.P., 2011. The X-ray fluorescence microscopy beamline at the Australian synchrotron. Paper Presented at the AIP Conference Proceedings.
- Pessi, I.S., Rutanen, A., Hultman, J., 2022. *Candidatus Nitrosopolaris*, a genus of putative ammonia-oxidizing archaea with a polar/alpine distribution. *FEMS Microbes* 3.
- Power, I.M., Wilson, S.A., Small, D.P., Dipple, G.M., Wan, W., Southam, G., 2011. Microbially mediated mineral carbonation: roles of phototrophy and heterotrophy. *Environ. Sci. Technol.* 45, 9061–9068.
- Power, I.M., Wilson, S.A., Dipple, G.M., 2013. Serpentinite carbonation for CO<sub>2</sub> sequestration. *Elements* 9, 115–121.
- Quast, C., Pruesse, E., Yilmaz, P., Gerken, J., Schweer, T., Yarza, P., Peplies, J., Glöckner, F.O., 2013. The SILVA ribosomal RNA gene database project: Improved data processing and web-based tools. *Nucleic Acids Res.* 41, 590–596.
- Rackley, S.A., 2017. Overview of carbon capture and storage. *Carbon Capture and Storage*, pp. 23–36.
- Ripka, R., Deruelles, J., Waterbury, J.B., Herdman, M., Stainer, R.Y., 1979. Generic assignment, strain histories and properties of pure cultures of cyanobacteria. *J. Gen. Microbiol.* 111, 1–61.
- Ruiz, F., Perlatti, F., Oliveira, D.P., Ferreira, T.O., 2020. Revealing tropical Technosols as an alternative for mine reclamation and waste management. *Minerals* 10, 110.
- Ryan, C.G., Siddons, D.P., Kirkham, R., Li, Z.Y., de Jonge, M.D., Paterson, D.J., Kuczewski, A., Howard, D.L., Dunn, P.A., Falkenberg, G., Boesenber, U., De Geronimo, G., Fisher, L.A., Halfpenny, A., Lintern, M.J., Lombi, E., Dyl, K.A., Jensen, M., Moorhead, G.F., Cleverley, J.S., Hough, R.M., Godel, B., Barnes, S.J., James, S.A., Spiers, K.M., Alfeld, M., Wellenreuther, G., Vukmanovic, Z., Borg, S., 2014. Maia X-ray Fluorescence Imaging: Capturing Detail in Complex Natural Samples. Paper Presented at the Journal of Physics: Conference Series.
- Sadowsky, M.J., Graham, P.H., 1998. Soil biology of the Rhizobiaceae. *The Rhizobiaceae: Molecular Biology of Model Plant-associated Bacteria*, pp. 155–172.
- Siddons, D.P., Kirkham, R., Ryan, C.G., De Geronimo, G., Dragone, A., Kuczewski, A.J., Li, Z.Y., Carini, G.A., Pinelli, D., Beuttemuller, R., Elliott, D., 2014. Maia X-ray microprobe detector array system. *Journal of Physics: Conference Series* (Vol. 499, No. 1, p. 012001). IOP Publishing.
- Southam, G., 2012. Minerals as substrates for life: the prokaryotic view. *Elements* 8 (2), 101–106.
- Sparks, R.S.J., 2013. Kimberlite Volcanism. *Annu. Rev. Earth Planet. Sci.* 41, 497–528.
- Wilson, S.A., Dipple, G.M., Power, I.M., Thom, J.M., Anderson, R.G., Raudsepp, M., Gabites, J.E., Southam, G., 2009. Carbon dioxide fixation within mine wastes of ultramafic-hosted ore deposits: examples from the Clinton Creek and Cassiar chrysotile deposits, Canada. *Econ. Geol.* 104, 95–112.
- Xiaofang, L., Huang, L., 2014. Toward a new paradigm for tailings phytostabilization – nature of the substrates, amendment options and anthropogenic pedogenesis. *Crit. Rev. Environ. Sci. Technol.* 45, 813–839.
- Yang, Y., Yang, J., Wu, W.M., Zhao, J., Song, Y., Gao, L., Yang, R., Jiang, L., 2015. Biodegradation and mineralization of polystyrene by plastic-eating mealworms: part 2. Role of gut microorganisms. *Environ. Sci. Technol.* 49 (20), 12087–12093.